

## Heat Flux Estimates for the Western North Atlantic. Part II: The Upper-Ocean Heat Balance\*

KATHRYN A. KELLY

*Department of Physical Oceanography, Woods Hole Oceanographic Institution, Woods Hole, Massachusetts*

BO QIU

*Department of Oceanography, University of Hawaii at Manoa, Honolulu, Hawaii*

(Manuscript received 26 April 1994, in final form 9 March 1995)

### ABSTRACT

The assimilation of temperature and altimetric velocity into a numerical model of the upper-ocean mixed layer in Part I allowed an analysis of the upper ocean heat budget for the western North Atlantic Ocean over the 2.5-year period of the Geosat Exact Repeat Mission (November 1986–April 1989). The balance of terms varied regionally: south of the Gulf Stream advection was relatively unimportant in the heat budget, and the ocean responded passively to changes in surface flux. Within the Gulf Stream and to the north of it, cooling of the upper ocean by advection was as large as  $0.15^{\circ}\text{C}/\text{day}$  for periods of several weeks. An analysis of the advection term showed that cooling by Ekman transport was opposed by warming from the geostrophic currents of the Gulf Stream, with cooling typically stronger by a factor of 2 because nonuniform Ekman transport disrupted the normal alignment between isotherms and sea surface height contours. There is a complex ocean–atmosphere coupling in this region: in addition to its increase during strong wind events, warming by geostrophic currents is a function of the strength of the Gulf Stream and its recirculation gyres. Over the 2.5-year period, the winds became progressively stronger, causing an increase in cooling by Ekman transport. Advective cooling was balanced by an increasingly positive surface flux (warming of the ocean by the atmosphere) at the rate of about 20% of the annually averaged surface flux per year. This positive trend in the surface flux was also observed in the estimates from the atmospheric general circulation model of the ECMWF.

### 1. Introduction

One of the fundamental ways in which the ocean and the atmosphere are coupled is through the transfer of heat across the air–sea interface. The idea that the mid-latitude ocean could force changes in weather patterns originated with the work of Namias (1959, 1963), who observed a correlation between sea surface temperature (SST) anomalies and storm tracks over the North Pacific Ocean. A subsequent analysis by Davis (1976) of sea level pressure and SST patterns suggested that the midlatitude oceans respond to atmospheric changes, rather than force the atmosphere, on timescales of months to years. Consistent with the idea that the atmosphere forces the ocean, the “anticyclogenesis” mechanism proposed by Worthington (1976) attributed an increase in volume transport in the Gulf Stream

to oceanic heat loss from cold continental air moving offshore in the winter. Adamec and Elsberry (1985) examined the effect of cooling events on a numerical model of the Gulf Stream and found that the cooling had less of an effect than changes in an alongstream wind stress, which caused the jet to be displaced southward. A recent reexamination of Worthington’s hypothesis by Huang (1990) suggested that the vertical mixing of momentum after a cooling event would reduce surface currents at the same time that the volume transport increased, which suggests that the surface response might appear quite different than the response below the mixed layer.

The history of the study of the air–sea interactions in the midlatitude ocean was summarized by Frankignoul (1985), who showed that a specified surface flux from the ocean could produce a definite, if somewhat weak, response by the atmosphere. Frankignoul suggested that the problem in determining the response of the atmosphere to the ocean was that the magnitude of the surface flux anomaly caused by a given SST anomaly was not known. More recently Cayan (1992) showed that over most of the midlatitude oceans, changes in wintertime ocean temperature could be predicted from the surface flux, even if the effect of anom-

---

\* Woods Hole Oceanographic Contribution Number 8717.

---

Corresponding author address: Dr. Kathryn A. Kelly, Department of Physical Oceanography, Woods Hole Oceanographic Institution, Woods Hole, MA 02543.  
E-mail: kkelly@whoi.edu

alous SST on the surface flux estimate was removed. However, the SST was not predictable in the summertime. Numerical simulations by Kushnir and Lau (1992), using a SST anomaly, showed a relatively weak response by the atmosphere that depended both on the sign of the anomaly and its timescale.

Studies of longer records of oceanic and atmospheric variables, as part of the National Oceanic and Atmospheric Administration's Atlantic Climate Change Program, suggest that the northwest Atlantic Ocean may actively participate in the coupling on decadal timescales. Deser and Blackmon (1993) showed an anomalous SST pattern in the vicinity of the Gulf Stream that was not correlated with (and therefore presumably not forced by) variations in the wind. Kushnir (1994) showed that the patterns of correlation between SST and winds at the decadal timescale were distinctly different from those at the interannual timescale and suggested that the SST anomalies preceded the wind anomalies.

The heat budget in the northwest Atlantic Ocean is critical in understanding global air-sea interaction because some of the largest surface heat fluxes in the World Ocean occur in the vicinity of the Gulf Stream (Isemer and Hasse 1987). Over much of the midlatitude oceans, the annually averaged flux of heat is from the atmosphere to the ocean. However, over the warm core of the Gulf Stream, which rapidly advects warm tropical water northward along the east coast of North America, the net surface flux of heat is from the ocean to the atmosphere. The large contribution of the Gulf Stream to the annual mean surface flux suggests that low-frequency changes in the intensity of the Gulf Stream could change the magnitude of that flux. This would indicate a forcing of the atmosphere by the ocean. Greatbatch et al. (1991), using historical hydrographic data, estimated that there were fluctuations of 30% in the strength of the Gulf Stream circulation between the early 1950s and the early 1970s. They compared differences in bottom pressure torques with differences due to wind stress and found the bottom pressure torque effects were much larger. On shorter timescales, Gulf Stream fluctuations have been observed by Zlotnicki (1990), Lillibridge and Cheney (1990), and by Kelly (1991) using the Geosat radar altimeter, which measures the height of the sea surface and from which geostrophic surface currents can be inferred (Fig. 1). Fluctuations in the sea surface height (SSH) difference across the Gulf Stream, which is a measure of the surface transport of the current, of up to 30% were observed using the Geosat altimeter data with periods of about 9 months between about 54° and 63°W (Kelly 1991). A trend, which decreased the mean SSH difference by about 9% over the 2.5-year Geosat Exact Repeat Mission (ERM: November 1986–April 1989), was also observed. Similar fluctuations have been observed in the Kuroshio Extension (Qiu et

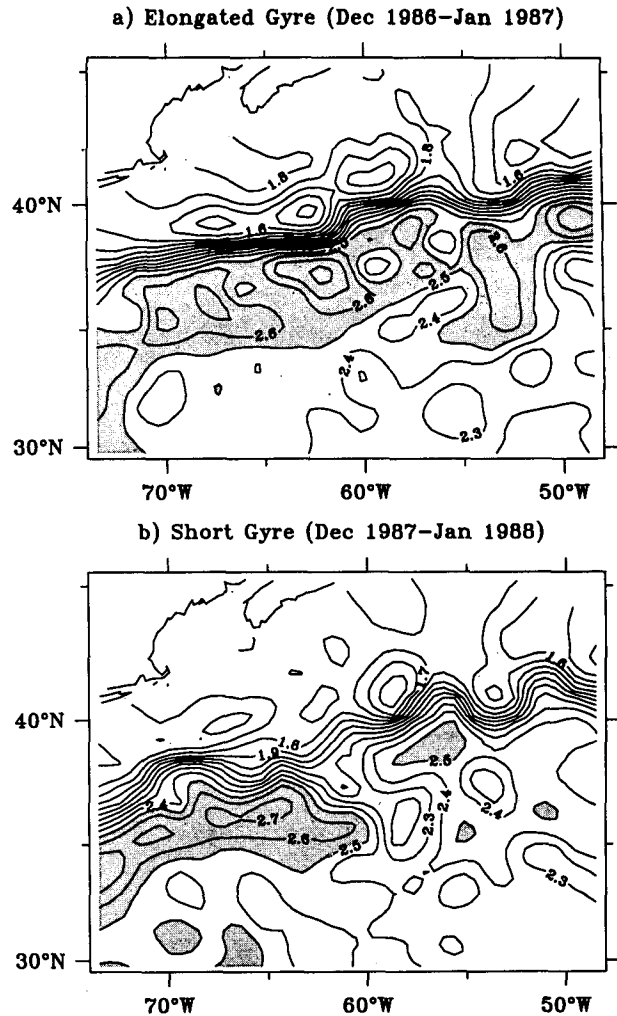


FIG. 1. Changes in Gulf Stream circulation. Maps of the sea surface height in the study area, averaged over four weeks for (a) Dec 1986–Jan 1987 and (b) Dec 1987–Jan 1988. SSH anomalies larger than 2.5 m are stippled to highlight the changes in the recirculation gyre south of the Gulf Stream. Although these fluctuations in Gulf Stream strength represent extreme conditions over the 2.5-year period, there was a trend from an elongated recirculation gyre, as in (a), to a short gyre, as in (b).

al. 1991), but with a trend toward increasing current strength over the same time period.

To study the changes in the upper ocean heat balance in response to realistic fluctuations in the Gulf Stream strength, a numerical model of the upper ocean mixed layer (Qiu and Kelly 1993, hereafter QK) in the North Atlantic was combined with satellite-derived SST and velocities from the altimeter (Qiu 1994). The simple mixed layer model included vertical entrainment of the cold water beneath the mixed layer and heating by the surface flux, as well as diffusion and advection. The recent availability of synoptic velocity and temperature fields from satellites has made the inclusion of the last two terms possible. The importance of advection was

shown in an analysis of the seasonal heat budget in the Kuroshio Extension using the same mixed layer model and forced by ECMWF surface flux estimates: cooling by advection offset nearly 30% of the surface warming due to the atmosphere (QK).

In contrast with the study in the Kuroshio Extension, the mixed layer model and observed SST in the Gulf Stream were used to estimate the surface flux, rather than predicting mixed layer temperature. The net surface flux was estimated as the residual of the heat budget, after subtracting the effects of entrainment, diffusion, and advection from the observed change in mixed layer temperature. Because of the relatively large errors in both the SST and in the advection terms, a Kalman filter was used to estimate surface flux from the time rate of change of SST, as described in Part I.

In this part of the analysis we analyze the heat budget over the whole domain and for subregions in section 2. The effect of fluctuations in Gulf Stream transport is described in section 3. We evaluate the accuracy of the surface flux estimates in section 4, followed by a discussion of the implications of trends in the terms in section 5. The results are summarized in section 6.

## 2. The upper ocean heat budget

A series of experiments were performed using the mixed layer model and assimilating temperature data as described in Part I. The estimate of the upper ocean heat budget described here is based on one of these experiments, for which an assessment of the surface flux estimates is given in section 4. With the exception of the early spring, agreement between the different surface flux estimates suggests that fields generated by assimilating data into the model can be used to understand the upper ocean heat budget. Ideally the heat budget analysis should be done using the heat content; however, because we have modeled only the mixed layer and that layer is not a material surface, mass is not conserved in the model. Therefore, the heat budget will be analyzed, as in QK, in terms of the contribution of the various terms to the temperature tendency equation

$$\frac{\partial T_m}{\partial t} + \frac{U}{h_m} \frac{\partial T_m}{\partial x} + \frac{V}{h_m} \frac{\partial T_m}{\partial y} = A_T \nabla^2 T_m + \frac{Q_{\text{net}} - q(-h_m)}{c_p \rho_0 h_m} - \Delta T \frac{w_e}{h_m}, \quad (1)$$

where  $T_m$  is the mixed layer temperature;  $U$ ,  $V$  are the horizontal transports in the mixed layer;  $h_m$  is the mixed layer depth;  $c_p$  the specific heat of water;  $\rho_0$  the reference density;  $A_T$  the subgrid-scale eddy diffusivity;  $Q_{\text{net}}$  the net heat flux through the ocean surface; and  $w_e$  is the vertical entrainment velocity into the mixed layer. The downward radiative heat flux at the bottom of the mixed layer,  $q(-h_m)$ , is included to account for possible penetration through the shallow mixed layer in

summer. The temperature difference between the mixed layer and the water below,  $\Delta T$ , was taken as fixed at  $0.5^\circ\text{C}$ . The transports are the sum of the surface geostrophic and the Ekman components and include a shear correction based on the mixed layer temperature gradients.

First, we present an analysis of the terms spatially averaged over the entire model domain and then break the analyses down into regions: south of the Gulf Stream, north of the Gulf Stream, and in the Gulf Stream. These regions were defined by examining the mean SST map for the period of observation. The northern region was defined as all those points where the mean SST was less than  $14^\circ\text{C}$  (Fig. 2); the Gulf Stream as the region between  $14^\circ$  and  $21.5^\circ\text{C}$ ; and the southern region as the region in which the mean SST exceeded  $21.5^\circ\text{C}$ .

### a. Entire region

Over the entire region, the dominant terms in the temperature equation (1) are the temperature tendency and the surface heating term  $Q/h_m$  (Fig. 3a). An error estimate for this term, as a function of time, is shown in Part I, Fig. 13c. The absolute magnitude of the error in  $Q/h_m$ , averaged over the entire region, is about  $0.015^\circ\text{C}/\text{day}$ . This error can also be interpreted as the residual in closing the upper ocean heat budget. The next largest term is that of advection, which is predominately negative, with intense cooling events in the spring of up to  $-0.04^\circ\text{C}/\text{day}$ . Entrainment contributes large values, greater than  $-0.01^\circ\text{C}/\text{day}$ , in the fall and winter (Fig. 3b), and the loss of heat through the bottom of the mixed layer reaches values of  $-0.01^\circ\text{C}/\text{day}$  in the summer, when the mixed layer is quite shallow.

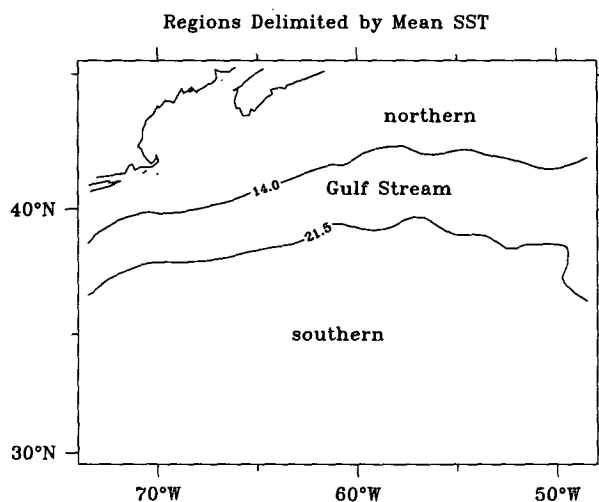


FIG. 2. Subdomains of the numerical mixed layer model for interpretation of the heat balance. The three regions are based on the mean SST: north of the Gulf Stream, in the Gulf Stream, and south of the Gulf Stream.

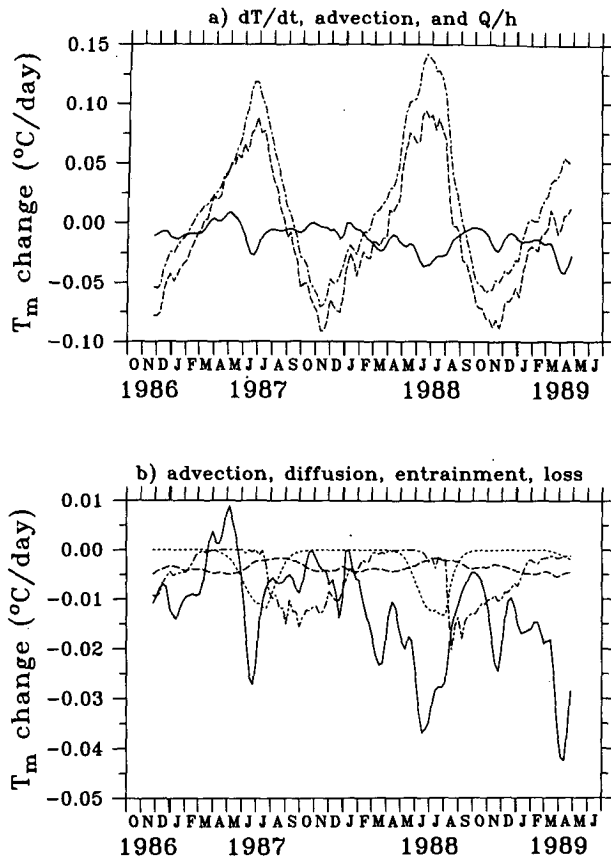


FIG. 3. Upper ocean heat balance averaged over the entire model domain. (a) Dominant terms of the heat balance: temperature tendency (dash-dot),  $Q/h_m$  (dashed), and advection (solid line). (b) Smaller terms of the heat balance: advection (solid line), entrainment (dash-dot), diffusion (dash), and heat loss (short dash).

Diffusion is always negative, with magnitudes less than  $0.005^\circ\text{C}/\text{day}$ . Note that diffusion is somewhat less important here than in a previous analysis of the Kuroshio Extension (QK), because the value of the diffusion parameter is substantially less (see discussion in Part I).

#### b. South of the Gulf Stream

In the large region south of the Gulf Stream, the contributions of advection and diffusion (not shown) are almost negligible because of the small temperature gradients there. The contribution of vertical entrainment is about the same as for the region as a whole. The overall balance is essentially that suggested by Cayan (1992) for a passive ocean response: the net surface flux can be used to predict the mixed layer temperature (Fig. 4).

#### c. North of the Gulf Stream

The northern region is quite different from the region south of the Gulf Stream: discrepancies between tem-

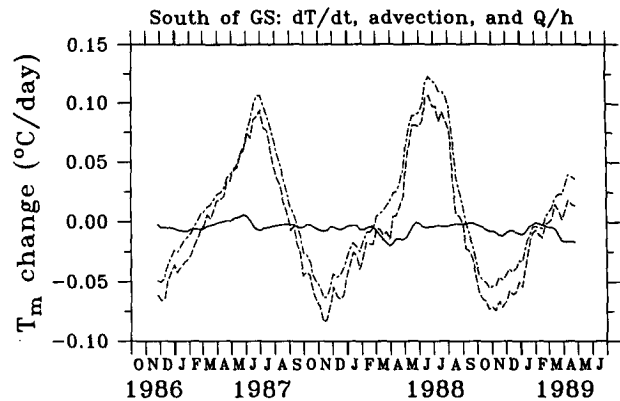


FIG. 4. Dominant terms in the upper ocean heat balance for the region south of the Gulf Stream. Temperature tendency (dash-dot) is nearly balanced by  $Q/h_m$  (dashed), with a relatively small contribution from advection (solid line).

perature tendency and net surface heating can be as large as  $0.10^\circ\text{C}/\text{day}$  (not shown). Of the other terms (Fig. 5a), advection dominates, with cooling events larger than  $-0.12^\circ\text{C}/\text{day}$  in the late spring (June 1987

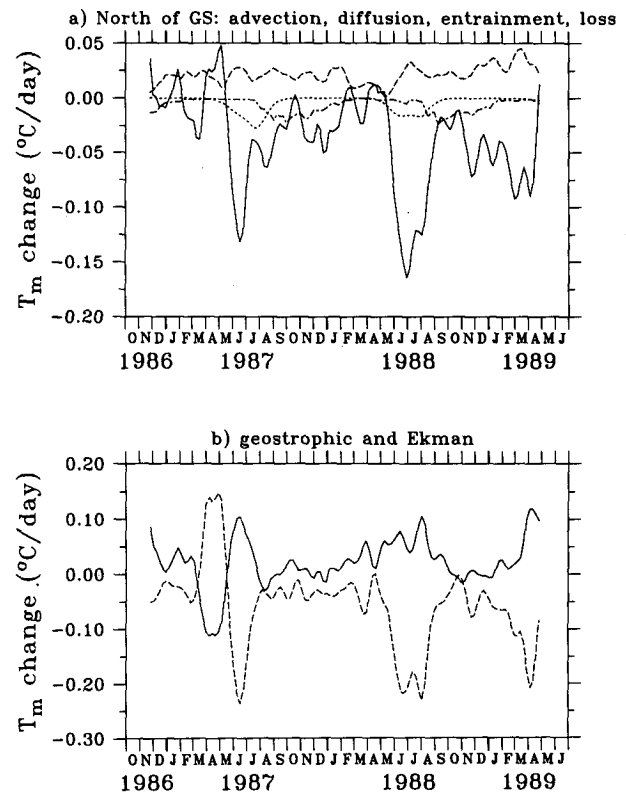


FIG. 5. Upper ocean heat balance north of the Gulf Stream. (a) Smaller terms of the heat balance: advection (solid line), entrainment (dash-dot), diffusion (dash), and heat loss (short dash). (b) Advection divided into its components: geostrophic (solid) and Ekman (dash).

and 1988), when the mixed layer is shallow and winds are strong. The intense cooling event in June 1987 was preceded by a smaller warming event in April/May; however, this event may be an artifact of the early mixed layer shoaling in the model, as discussed in section 4, because the Ekman velocity is inversely proportional to the mixed layer depth.

The advection and diffusion terms are a factor of 10 larger than in the southern region, and diffusion is generally positive, indicating warming by the nearby Gulf Stream. Entrainment, which begins in August and ends by March, has the same magnitude as in the southern region. Heat loss through the bottom of the mixed layer is substantial, but small relative to advection.

It is instructive to divide the advection into the geostrophic and Ekman components (Fig. 5b). There is a clear trend in the advection toward more cooling in the northern region, which is due to the Ekman transport (Fig. 5b). The Ekman component is generally negative, corresponding to southward flow in response to eastward wind stress. The geostrophic component is nearly always positive (except when the Ekman contribution is positive due to westward winds, as in April 1987), so that it opposes the effect of the Ekman component. What causes this opposition? In the absence of strong winds, geostrophic contours and the isotherms are generally aligned, consistent with a thermal wind balance, resulting in a small advection contribution. When the winds are strong and not uniform over the region, the advection by Ekman transport disrupts this alignment in the Ekman layer (synonymous here with the mixed layer), and the geostrophic currents attempt to restore it, resulting in relatively large advection terms of both signs.

#### d. In the Gulf Stream

The balance of terms in the Gulf Stream itself is similar to that in the northern region: departures from a balance between temperature tendency and net surface heating can be as large as  $0.10^{\circ}\text{C}/\text{day}$ . Advection is somewhat smaller in magnitude than that of the northern region with similar events (Fig. 6a). As in the northern region, there is a trend in the advection toward more cooling. Diffusion is approximately the same magnitude (Fig. 6a), but negative, indicating cooling by the slope water. The heat loss is smaller and entrainment is about the same. A close examination of the advection terms in the Gulf Stream (Fig. 6b) shows that the cooling trend is apparently due to an increase in the contribution of the Ekman component, but there is also a contribution from weakening geostrophic currents. The cooling by the Ekman component is often nearly balanced by the warming due to the Gulf Stream; however, in June of 1987 and 1988 and particularly in April 1989, the cooling overwhelms the warming.

This trend in advection is also apparent in the balance for the entire region and is offset by a trend in the

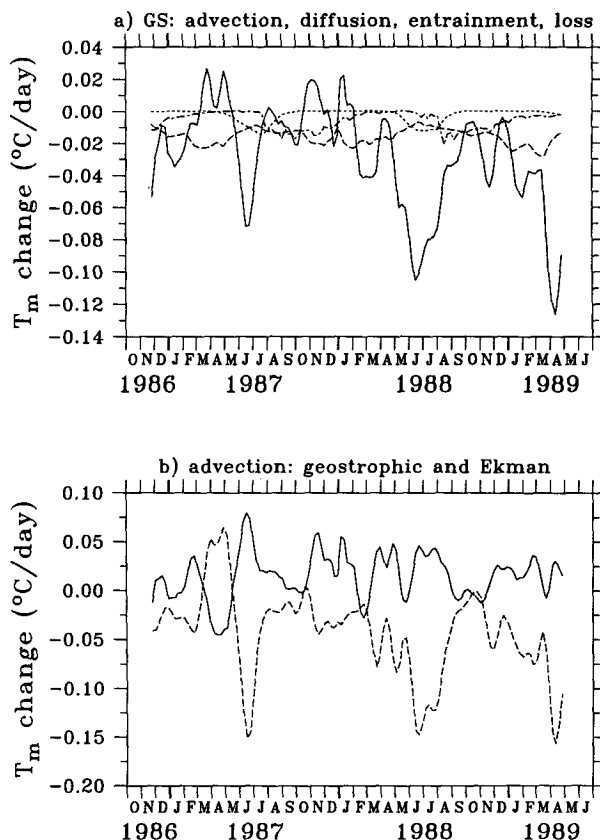


FIG. 6. Upper ocean heat balance in the Gulf Stream. The quantities shown are defined in Fig. 4. Note the cooling trend of advection in (a), which is caused by a combination of an increase in Ekman advection and a decrease in the geostrophic advection, shown in (b).

net surface heating term, because the temperature tendency has no significant trend. These trends can best be seen by removing the first two harmonics of the annual signal from each of the terms (Fig. 7). The trend in temperature tendency (not shown) is  $-0.0016^{\circ}\text{C}/\text{day}$  per year, compared with trends for  $Q/h_m$  and advection of  $0.0067^{\circ}$  and  $-0.0086^{\circ}\text{C}/\text{day}$  per year, respectively. There is a corresponding change in the net surface heat flux  $Q_{\text{net}}$ , which amounts to about  $15 \text{ W m}^{-2}$  per year.

### 3. The contribution of GS transport fluctuations

The relationship between changes in the gyre structure (Fig. 1) and the heat budget is complicated by the fact that the heat budget has a large seasonal component, whereas the current fluctuations have a slightly higher dominant frequency. To see whether the cooling trend in advection (Fig. 6b) is related to a weakening of the Gulf Stream in the eastern part of the region, which can be seen in the nonseasonal SSH difference across the Gulf Stream (Fig. 8), we compared a measure of the gyre structure with a measure of geostrophic

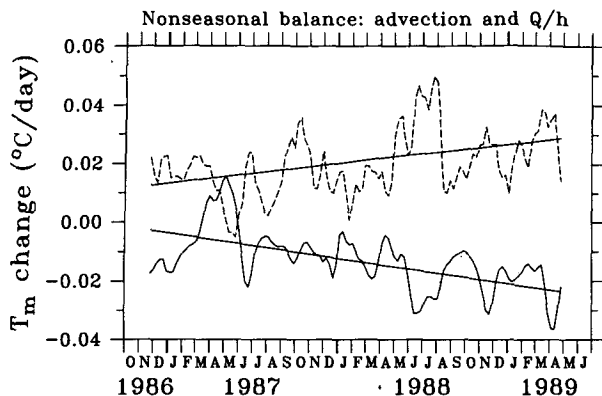


FIG. 7. Nonseasonal advection and heating terms. After removing the annual and semiannual harmonics from both the advection term and  $Q/h_m$ , the negative trend in advection (solid line) can be seen to nearly balance the positive trend in  $Q/h_m$ . The solid lines are the best fit to a linear trend. Figure 11. Nonseasonal SSH differences across the Gulf Stream. After removing the relatively small annual and semiannual harmonics from the SSH differences, the Gulf Stream west of  $63^\circ$  (solid line) shows no apparent trend, whereas the Gulf Stream east of  $63^\circ$  (dashed line) decreases in strength by about 9% over a 2.5-year period.

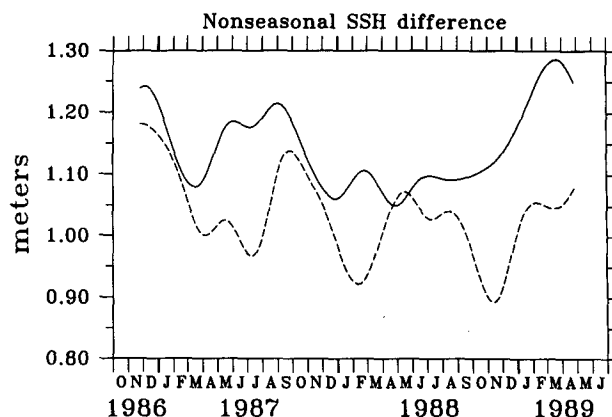


FIG. 8. Nonseasonal SSH differences across the Gulf Stream. After removing the relatively small annual and semiannual harmonics from the SSH differences, the Gulf Stream west of  $63^\circ$ W (solid line) shows no apparent trend, whereas the Gulf Stream east of  $63^\circ$ W (dashed line) decreases in strength by about 9% over the 2.5-year period. A small SSH difference in the eastern region relative to the SSH difference in the western region suggests a short recirculation gyre as in Fig. 1b.

advection. The SSH maps in Fig. 1 represent extremes (cf. Fig. 8) in the gyre structure; however, there was also a trend from a stronger jet (Fig. 1a) east of  $63^\circ$ W to a weaker one (Fig. 1b). The ratio of the SSH difference in the eastern region to the SSH difference in the western region can be used to characterize the recirculation gyre pattern: a high ratio suggests the elongated gyre in Fig. 1. The effectiveness of the geostrophic transport in opposing Ekman advection can also be characterized by a ratio: that of (minus) the geostrophic advection to the Ekman advection. The ratio is used, rather than just the geostrophic advection itself, because, as mentioned in the previous section, significant geostrophic advection only occurs when Ekman transport disrupts the alignment between isotherms and geostrophic contours. The effect of the recirculation gyre pattern on advection can be seen by plotting the weekly advection ratios against the SSH difference ratios (Fig. 9). Although there is considerable scatter, there is a clear tendency for the elongated gyre (large SSH ratio) to be more effective (large advection ratio) in opposing cooling. The correlation between the ratios is marginally significant at 0.44. Note that the ratio was only computed for Ekman advection terms larger than  $0.02^\circ\text{C}$  per day.

#### 4. Evaluation of the surface flux estimates

In addition to deriving an error estimate from the Kalman filter, discussed later in this section, we attempted to assess the accuracy of our estimates of the net surface flux  $Q_{\text{net}}$  by comparison with the estimates from the atmospheric circulation model of the ECMWF and with the Bunker climatological esti-

mates. Comparing the spatially averaged estimate of  $Q_{\text{net}}$  from the Kalman filter with that from the ECMWF, we note that there are two basic discrepancies (Fig. 10).

The first discrepancy in the estimates occurs in February/March, when the Kalman estimates become positive nearly two months earlier than the ECMWF estimates. The ECMWF estimates are more consistent with climatological estimates (Isemer and Hasse 1987), which suggest surface flux should be slightly negative through April. The Kalman surface flux estimates gen-

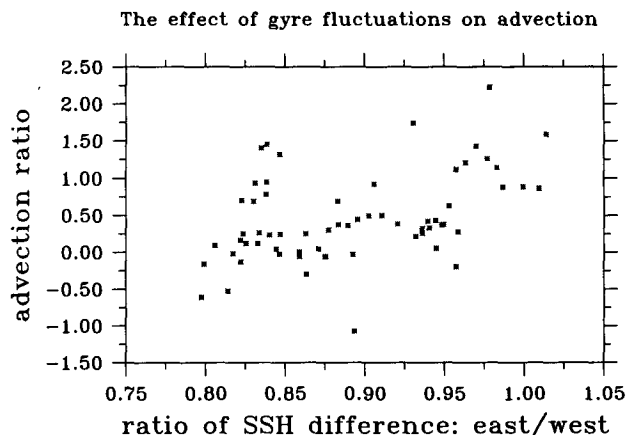


FIG. 9. The effect of the Gulf Stream circulation on advection. The ratio of the weekly estimates of warming by geostrophic advection to the cooling by Ekman transport is plotted against a measure of the elongation of the recirculation gyre (Fig. 1): the ratio of mean SSH difference east of  $63^\circ$ W to mean SSH difference west of  $63^\circ$ W. The trend suggests that an elongated gyre warms the Gulf Stream region more effectively than a short gyre.

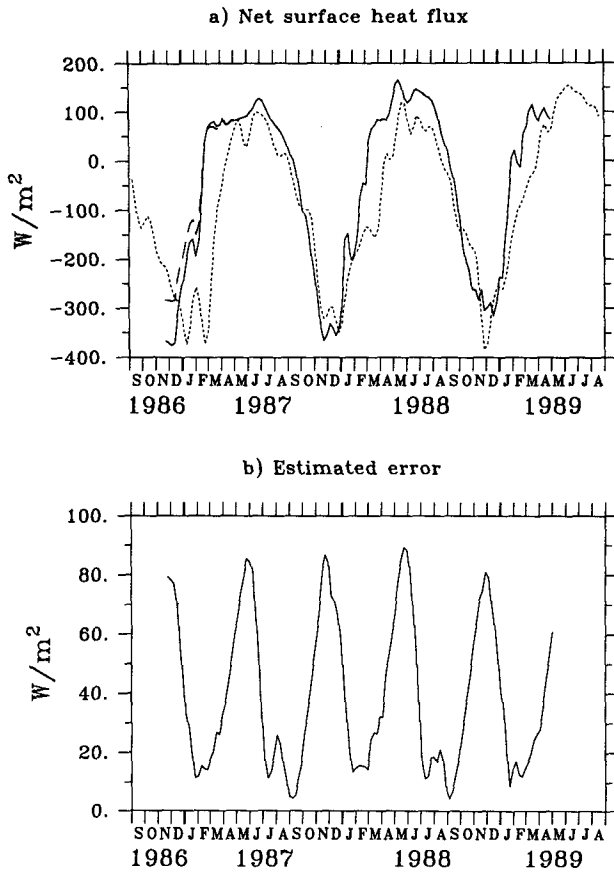


FIG. 10. Net surface flux estimates from the mixed layer model and from ECMWF. (a) Spatially averaged estimates of the net surface flux from the Kalman filter (solid line) and ECMWF (dashed line) and (b) an error estimate for the Kalman filter estimate. The larger (more negative) fluxes in the fall of 1986 resulted from initializing the model with the Nov 1987 mixed layer depth, rather than with a climatological estimate.

erally become positive when the temperature tendency in the data becomes positive; therefore, we first examine the accuracy of the temperature data.

There are systematic differences between the temperature data and the climatological mixed layer temperature (Levitus 1982; Fig. 11). The data are nearly  $2^{\circ}C$  warmer than the climatological mixed layer temperatures, and the seasonal range of temperature is more than  $1^{\circ}C$  larger (Fig. 11a). As discussed in Part I, section 4, these temperature data have already been corrected for typical seasonal differences between an in situ SST measurement and the mixed layer temperature, using the Levitus data. This correction had little effect on the surface flux estimates because the temporal derivative of the correction was small. There are also significant differences between the temperature tendency computed from the corrected data and from the Levitus climatology (Fig. 11b), which are comparable in size with the estimates of the error in  $Q/h_m$

from the Kalman filter. In both 1987 and 1989 there are periods of positive temperature tendency beginning in late February, a month earlier than in the climatological estimates. In 1988 the temperature tendency is more positive than the climatology, beginning in late March. These differences could account for about one month of the discrepancy between the Kalman estimates and the climatological surface flux. The discrepancy in temperature tendency could be due to systematic errors in the AVHRR SST, or it could be due to interannual variations in temperature.

Although this difference in temperature tendency can explain a difference of nearly one month in the phase of the Kalman estimates relative to climatology, the Kalman estimates also lead the ECMWF estimates by nearly two months in the spring. One possible explanation is that the ECMWF model is not sufficiently sensitive to interannual SST differences, and thus it produces flux estimates rather close to the climatolog-

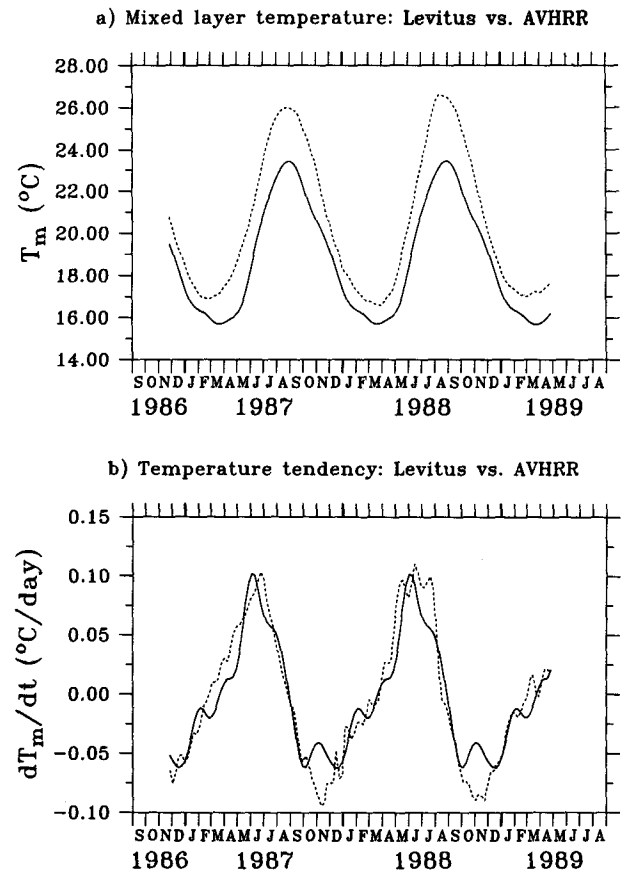


FIG. 11. Mixed layer temperature and temperature tendency. (a) Climatological mixed layer temperature (solid line) and mixed layer temperature estimated from AVHRR data (dashed line). (b) The temporal derivative of climatological temperature (solid) and the AVHRR-derived temperature (dashed). Note that the temperature tendency from the AVHRR data becomes positive earlier in the spring than the climatological value.

ical values. This view is supported by modeling studies by Y. Kushnir (1994, personal communication), which suggest that atmospheric global circulation models underrespond to SST anomalies.

Alternatively, there may be a systematic cooling bias in the mixed layer model, which causes the surface flux estimate to be too positive. In Part I, we assumed that there was a mean error in advection and derived a mean SSH correction, which decreased the cooling due to advection. This correction assumed that the mean advection error was due to geostrophic advection. The error may instead be due to an overestimate of the wind stress, which in turn leads to an overestimate of cooling by Ekman transport. An experiment with wind stress reduced by 30% gave correspondingly smaller values for the Ekman advection but did not affect the phase of the surface flux estimates, nor substantially reduce the surface flux estimates in the summer. However, a systematic overestimate of wind stress, as suggested by Nuñez et al. (1994) for the ECMWF 1000-mb wind fields, would also have biased the tuning of the model parameters and would not be entirely corrected by reducing the wind stress afterward.

Besides advection, a possible source of error for this problem is the inability of the model to realistically simulate the formation of a new mixed layer in the spring, while the deep winter layer gradually erodes. This simple model requires a single mixed layer, which is everywhere spatially connected. To achieve a shallow mixed layer in the spring, the deep mixed layer must gradually shoal. As was discussed in Part I, it was necessary to limit the shoaling speed in this model to prevent numerical instabilities from the noisy surface flux estimates. However, this limitation is not a likely cause since the model mixed layer still shoals fairly rapidly (Fig. 12) and much earlier than in the climatological estimates.

Another discrepancy between the two estimates is the much more positive Kalman surface flux estimates in the first half of 1987 (Fig. 10). There are two possible sources for this discrepancy also. First, as was shown by Bates (1994), there was a calibration error in the AVHRR data in the first half of 1987, which made the AVHRR estimates too cold by about  $0.5^{\circ}$ – $1.0^{\circ}$ C at  $40^{\circ}$ – $50^{\circ}$ N. An empirical correction for this problem was applied to the data we used here, as described in Part I. The National Meteorological Center (NMC) SST product used by ECMWF is partially derived from AVHRR data (B. Barnier 1992, personal communication). The AVHRR data used in the NMC SST analysis would have contained these erroneous temperatures, although there may have been some correction based on available in situ data. The negative springtime surface flux estimates from ECMWF are consistent with colder SST, in the sense of an unseasonally late spring warming; however, the ECMWF model could also respond to colder SST by producing more positive fluxes.

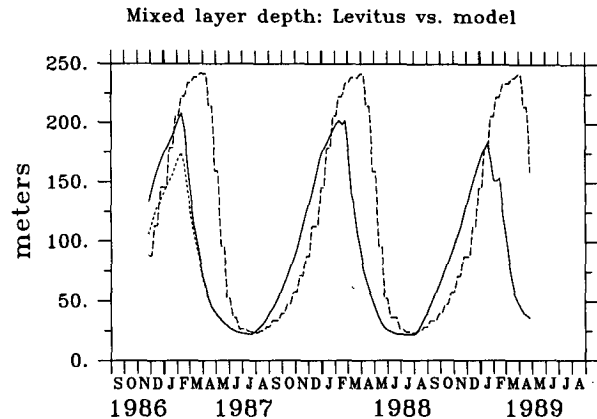


FIG. 12. Comparison of model estimates of mixed layer depth with Levitus climatology. Mixed layer depth for the model initialized with climatological mixed layer depths (short dash) and initialized with the Nov 1987 values (solid), compared with the climatological values (long dash).

Another source of error, which can be tested more easily, is the initialization of the mixed layer model. Originally, we initialized the model in November 1986 with the November climatological mixed layer depth from Levitus (1982), which was about 90 m, on average over the domain. In the two subsequent November mixed layer model gave depths of about 110 m (Fig. 12). This suggests that both deepening and shoaling of the mixed layer occur earlier in the model than in the climatological fields. Next, we initialized the model with the mixed layer depth from November of 1987 and reran the Kalman filter to get new surface flux estimates (Fig. 10). Note that we only constrain the ratio of  $Q/h_m$  so that a deeper mixed layer will result in a larger magnitude of the surface flux, with no corresponding effect on the temperature tendency. This deeper mixed layer gave a surface flux of about  $-380$   $W m^{-2}$  in late November, as compared with about  $-290$   $W m^{-2}$  using the Levitus mixed layer depth. However, the differences between the two estimates became negligible after about three months, which suggests that this was not the primary cause of the discrepancy in early 1987.

To derive an estimate of the error in the surface flux, we combined the Kalman filter error estimates with climatological estimates of the variables. The Kalman filter generates estimates of the ratio  $Q/h_m$ , where we have defined  $Q = Q_{net}/(\rho_0 c_p)$ , rather than for the surface flux  $Q_{net}$  alone. To derive an error estimate  $\delta Q$ , we note that

$$\delta \left[ \frac{Q}{h_m} \right] = \frac{\delta Q}{h_m} - \frac{Q}{h_m^2} \delta h_m \quad (2)$$

so that the error in  $Q$  is given by

$$\delta Q_{net} = c_p \rho_0 h_m \delta \left[ \frac{Q}{h_m} \right] + c_p \rho_0 \left[ \frac{Q}{h_m} \right] \delta h_m, \quad (3)$$

where  $\delta h_m$  is an error estimate for the mixed layer depth, a quantity which was not estimated by the model/Kalman filter. Errors in  $h_m$  include systematic errors in both the model and the climatology, and interannual variations. For an order of magnitude estimate we assumed that the  $h_m$  error can be represented as 20% of the difference between the model  $h_m$  and the climatological value. In addition, we need to know the actual value of  $Q/h_m$  and the error  $\delta[Q/h_m]$ , which was estimated by the Kalman filter and has a value of about  $0.015^\circ\text{C}/\text{day}$ . For the values of  $Q/h_m$  and  $h_m$  in (3), we used estimates of the annual cycle of these variables derived by fitting annual and semiannual harmonics to the weekly Kalman/model estimates over the 2.5-year period. This produced the error estimates for  $Q_{\text{net}}$  in Fig. 10b. Note that errors exceed  $100 \text{ W m}^{-2}$  in the winter when the mixed layer is deep and in the spring when the model mixed layer is systematically shallower than the climatology. Errors in the summer/fall are as low as  $20 \text{ W m}^{-2}$ . The Kalman estimates and the ECMWF estimates agree within these errors, except in February–March and in January–February 1987.

## 5. Discussion

Over most of the western North Atlantic, the dominant balance in the heat budget was between changes in mixed layer temperature and changes in the net surface flux. This is consistent with an analysis of the heat budget near Cape Hatteras during a single wintertime cold air outbreak. Xue et al. (1995) showed that the dominant balance was between changes in heat content and the net surface flux, analogous to what was shown here for the region south of the Gulf Stream. The authors concluded that over a period of several days, alongstream advection by the Gulf Stream could not compensate for the intense cooling by the atmosphere.

Although this was also the case here for most of the region, our analysis suggests that within the Gulf Stream and north of it, advection created a significant departure from a balance between temperature tendency and surface heating on timescales of weeks to years. The largest advection contribution was cooling by Ekman transport during strong wind events rather than from advection by geostrophic currents. These cooling events occurred primarily in the late spring when the mixed layer was shallow, and the effect was strongest far to the north and east of Cape Hatteras near the Grand Banks. Although within the Gulf Stream advection by geostrophic currents had the largest magnitudes, advection by Ekman transport makes a greater contribution when averaged spatially or temporally because of its larger spatial scales. The importance of advection by Ekman transport relative to advection by eddies was noted by Lentz (1987) for the northern California shelf. He showed that advection by eddies was not important if the heat budget was averaged over a region larger than the characteristic eddy size. In our

analysis, fitting the heat flux estimates to a few spatial modes in the Kalman filter is equivalent to spatial averaging and reduces the importance of advection by eddies on the heat flux estimates.

Nevertheless, larger-scale current fluctuations can make substantial contributions to the averaged heat budget, as was shown in section 3. Changes in the shape of the recirculation gyre structure, associated with changes in the strength of the eastward flowing Gulf Stream, were shown to affect the degree to which warming by geostrophic advection can compensate for cooling by Ekman transport. This compensation ranges from complete dominance of cooling by Ekman transport to a situation in which there is a net warming by geostrophic currents (Fig. 9). On average within the Gulf Stream, however, advection by Ekman transport is twice as large as advection by geostrophic currents.

We found the coupling between geostrophic and Ekman advection rather surprising; it appears to be due to the disruption in the alignment between isotherms and geostrophic contours by nonuniform Ekman transport. Generally, the temperature contours are aligned with the strong Gulf Stream currents and there is little temperature advection. However, strong nonuniform winds can disrupt this alignment, resulting in large contributions to advection. For example, if the Gulf Stream is entirely zonal, and winds blow toward the east, then Ekman transport will be uniformly southward, cooling the entire region uniformly, and advection by geostrophic currents will not affect the temperature. If instead, as is generally the case, eastward winds are stronger near the Grand Banks, then cooling by Ekman transport is more pronounced there, and there will be a zonal temperature gradient. Then, warmer water upstream will be advected downstream by the Gulf Stream. The amount of warming will depend both upon the magnitude of the zonal gradient and the strength of the Gulf Stream. This same coupling can be seen in a related study of the heat budget of the Kuroshio Extension (QK, their Fig. 11) where cooling and warming by Ekman transport are opposed by advection by the geostrophic currents in the jet core.

Potentially, then, there are two ways in which the ocean contributes to the net surface flux of heat: The first is by the intense cooling associated with Ekman transport in the vicinity of a strong temperature front. This may be the mechanism responsible for the correlation between SST and winds on the interannual timescale, as discussed by Kushnir (1994). The strength of the cooling is a complicated function of both magnitude and orientation of the wind stress relative to the temperature front as well as the depth of the Ekman layer (here, synonymous with the mixed layer depth).

The second mechanism is that of warming by large-scale geostrophic currents. This could be the mechanism that is responsible for the decadal-scale SST fluctuations, which are not correlated with wind stress (Deser and Blackmon 1993; Kushnir 1994). The pattern

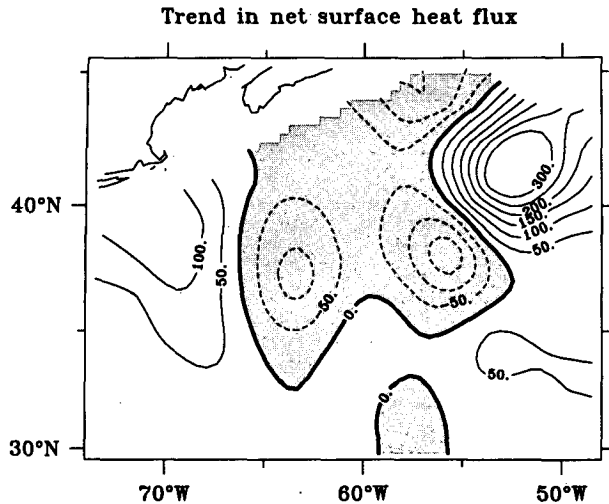


FIG. 13. The nonseasonal change in net surface flux between Nov 1986 and Apr 1989. Although on average there was a trend toward more positive surface fluxes, particularly in the northeastern part of the domain, the trend was negative (decreased warming of the ocean by the atmosphere) south of the Gulf Stream and west of 55°W.

of decadal SST variation found by Kushnir (1994) showed the distinctive pattern of the Gulf Stream path, which is consistent with the idea that the strongest temperature advection occurs near the temperature front. These gyre fluctuations have a trend over the 2.5 years (Fig. 8), which allows for the possibility of decadal timescales. However, this short time series is inadequate to resolve this issue, particularly because the combination of the higher-frequency fluctuations of the large-scale circulation and the seasonality of intense cooling events makes it virtually impossible to discern a trend in advection associated with the trend in the circulation. In addition, this analysis suggests that the geostrophic advection is associated with winds, in the sense that it becomes large only when there is also advection by Ekman transport.

The annual signal dominates in all of the terms in the heat budget; however, it is the interannual and longer variations that are of interest in understanding climate changes. Therefore, we removed both annual and semiannual fluctuations from the surface flux, mixed layer temperature, and wind stress to show the trends over the period of this study (Figs. 7, 8, and 13–15). The trend toward increased cooling from advection associated with a more positive surface flux (Fig. 7), that is, less flux of heat from the ocean to the atmosphere. Trends toward more positive surface flux in both estimates were significant: an increase in surface flux of about  $15 \text{ W m}^{-2}$  per year ( $12 \text{ W m}^{-2}$  for ECMWF), about 22% (18%) of the annual averaged surface flux. Over the 2.5-year period (November 1986–April 1989) this represents an approximately 50% increase in the annually averaged surface flux.

The spatial structure of the trend in surface flux is rather complex (Fig. 13): the trend is actually negative south of the Gulf Stream, with a region of strikingly large positive values in the northeast corner of the domain. This latter region had a relatively small positive value ( $<20 \text{ W m}^{-2}$ ) in the average over all of 1987, compared with a value of about  $150 \text{ W m}^{-2}$  in 1988. The increasing heat fluxes are compensating for cooling by Ekman transport due to increasing northeastward wind stress in this region (Fig. 15). By April 1989 the fluxes are unrealistically positive, which suggests that ECMWF wind stress magnitudes are too large. The surface flux south of the Gulf Stream changed from a minimum of about  $-150 \text{ W m}^{-2}$  in 1987 to about  $-200 \text{ W m}^{-2}$  in 1988.

The trend in mixed layer temperature has features similar to the surface flux, although there is no simple relationship between them (Fig. 14), because temperature changes are proportional to the ratio of the flux to the mixed layer depth. North of the Gulf Stream the sea surface was approximately  $1^\circ\text{C}$  colder at the end of the period than at the beginning, whereas the region south of the Gulf Stream was  $0.5^\circ\text{C}$  warmer. The region of increasing surface flux corresponds primarily to a region of decreasing temperature, which suggests that in this region the mixed layer depth is increasing. Similarly, the region of increasing temperature along the Gulf Stream path, centered at  $58^\circ\text{W}$ , corresponds to a region of decreasing surface flux, although there is no feature in the temperature trend corresponding to the decreasing surface flux centered at  $63^\circ\text{W}$ . This suggests that the robust correlations between surface flux and SST done by Liu and Gautier (1990) for the tropical Pacific would not hold here.

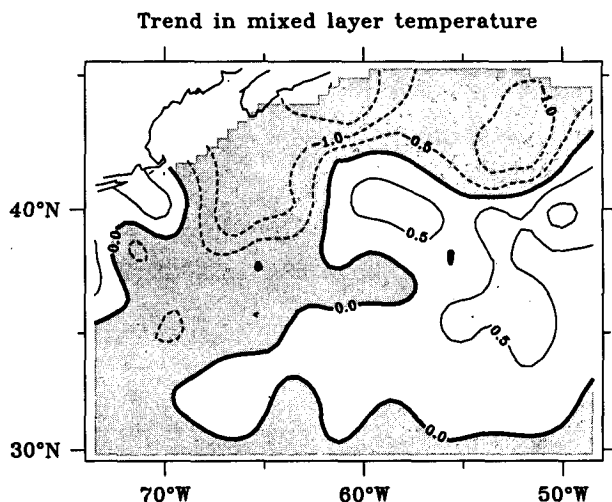


FIG. 14. The nonseasonal change in SST between Nov 1986 and Apr 1989. There was a cooling trend over the 2.5-year period of study over most of the model domain, with values of  $-0.5^\circ$ – $1.0^\circ\text{C}$ . However, south of the Gulf Stream, there was a net warming with values as large as  $0.5^\circ\text{C}$ .

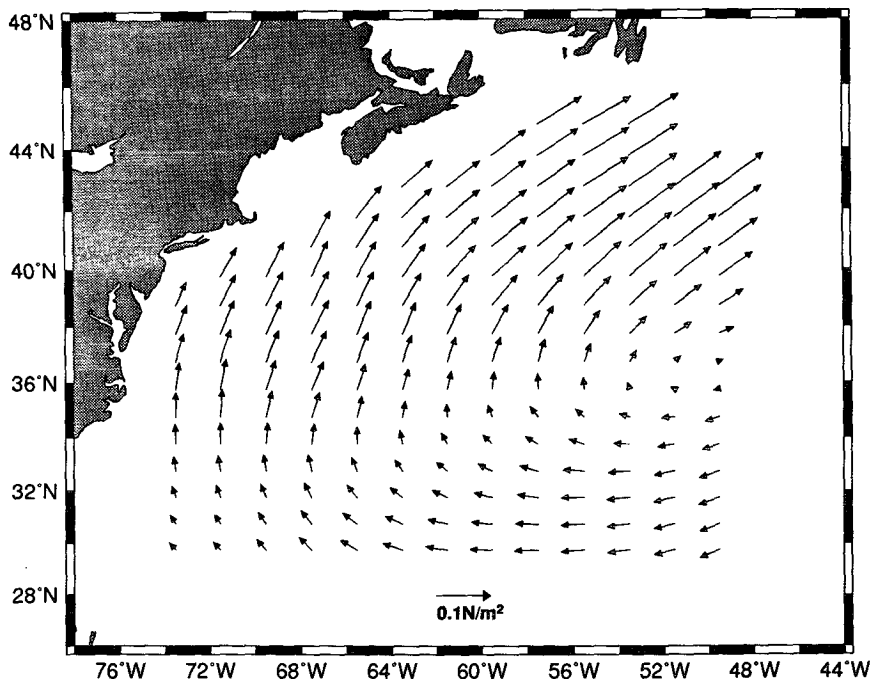


FIG. 15. The nonseasonal change in wind stress between Nov 1986 and Apr 1989. There was a trend toward stronger northeastward wind stress, particularly in the northeast corner of the domain.

Consistent with the temperature trend is a trend in the wind stress (Fig. 15), which shows an increase in the northeastward wind stress, particularly near the Grand Banks. This increase in wind stress undoubtedly caused the cooling trend in the Ekman advection (Figs. 5b, 6b). Although causality cannot be established, even statistically, using such a short time series, it seems most likely that changes in wind stress caused cooling by Ekman advection, which in turn caused the trend in the surface flux. The atmosphere and ocean appear highly coupled here, in that the cooling depends on the existence of the strong temperature front of the Gulf Stream.

What this study could not address was the relationship between changes in gyre circulation and the changes in meridional heat transport in the North Atlantic. There may be a connection between SST anomalies north of the study region and the intensity of the Gulf Stream because the Gulf Stream feeds into the North Atlantic Current, which flows northward east of Newfoundland. The transport of warm water by the North Atlantic Current plays an important role in the North Atlantic heat budget (Talley and McCartney 1982; McCartney and Talley 1984). However, to understand how changes in Gulf Stream circulation affect the transport of heat within the North Atlantic, it will be necessary to couple a mixed layer model with an interior ocean model. The relationship between the effects of advection in the

mixed layer and those below the mixed layer is not obvious, as noted by QK. For the Kuroshio Extension, the large meridional temperature gradients in the mixed layer, combined with the large Ekman transport, made cooling the dominant effect of advection near the surface. Below the mixed layer, where geostrophic advection dominates and meridional gradients are weaker, the dominant effect of advection may be to warm the region.

The Gulf Stream fluctuations may have important implications for biological processes. Recently correlations between Gulf Stream path fluctuations and plankton abundance in the North Sea were observed (Taylor et al. 1992). A suggested probable mechanism was changes in the storm tracks across the North Atlantic, associated with changes in the location of the Gulf Stream. However, it is not clear why a simple translation of the Gulf Stream of typically one degree of latitude would change weather patterns across the entire North Atlantic. The explanation may come from a correlation between the Gulf Stream path and changes in the gyre structure. An empirical orthogonal function (EOF) analysis of the SSH difference across the Gulf Stream and the Gulf Stream path (Kelly and Watts 1994) showed a correlation between an elongated gyre and a more northerly path relative to the short gyre. Thus, the Gulf Stream path changes may serve as a proxy for changes in the gyre structure. If, as hinted at in Fig. 9, these changes affect the upper ocean heat

budget, they may eventually influence the biological processes in the North Sea through the atmospheric response. However, numerical simulations of atmospheric circulation to date have shown only a relatively small response to surface flux anomalies of this magnitude (Frankignoul 1985; Kushnir and Lau 1992); however, recent simulations by Y. Kushnir (1994, personal communication) suggest that these atmospheric models may be underresponding to SST anomalies.

## 6. Summary and conclusions

The assimilation of temperature and velocity data into a numerical model of the upper ocean mixed layer, as described in Part I, allowed an analysis of the upper ocean heat budget from November 1986 to April 1989 and gave an estimate of the net surface flux for the western North Atlantic Ocean.

Over the entire region, the dominant terms in the temperature equation were the temperature tendency and the surface heating term, with the next largest term being advection. The balance of terms varied regionally: south of the Gulf Stream, temperature tendency balanced surface heating with other terms being negligible; north of the Gulf Stream and within it, advection by Ekman transport, especially in late spring, was as large as the average temperature tendency for the entire region. Within the Gulf Stream itself, advection by geostrophic currents was significant, with a magnitude of approximately half that of the Ekman advection. Warming by geostrophic currents was strongest during strong wind events and partially compensated for the cooling by Ekman transport: this increase in warming by geostrophic currents was apparently due to the disruption of the normal alignment between isotherms and geostrophic contours by nonspatially uniform Ekman transport.

The spatially averaged estimate of the surface flux from the model/Kalman filter agreed within the estimated errors with that from the ECMWF, with the exception of the months of February and March of each year, and of the first half of 1987. These discrepancies were attributed in part to the tendency of the SST derived from the AVHRR data to lead the climatological mixed layer tendency by a month.

There was a trend toward increased cooling from advection, which was accompanied by an increasingly positive surface flux, that is, more flux of heat from the atmosphere to the ocean. The trend toward more positive surface flux was significant: an increase in surface flux of about  $15 \text{ W m}^{-2}$  per year averaged over the entire domain, or about 22% of the annually averaged surface flux. A similar trend was observed in the ECMWF surface flux estimates. The increased cooling by advection was apparently caused by an increase in the eastward wind stress. This result suggested a complex atmosphere-ocean coupling on interannual time-scales: eastward wind stress causes intense cooling by

advection near the Gulf Stream, which in turn causes an increase in the surface heat flux. This coupling is modulated somewhat by fluctuations in the Gulf Stream circulation, with advection by geostrophic currents opposing the cooling by Ekman transport.

*Acknowledgments.* The authors would like to thank J. Price for helpful discussions regarding this analysis and S. Lentz for a careful reading of the manuscript. M. Caruso provided programming support for the data processing. This research was supported by the National Oceanographic and Atmospheric Administration through the Atlantic Climate Change Program under Contract NA16RC0468-01 and by the Office of Naval Research under Contract N00014-92-J-1656 (Kuroshio Extension Regional Experiment).

## REFERENCES

- Adamec, D., and R. L. Elsberry, 1985: Response of an intense ocean current system to cross-stream cooling events. *J. Phys. Oceanogr.*, **15**, 273–287.
- Bates, J., 1994: A decade of multispectral sea surface temperature observations from space. *Adv. Space Res.*, **14**(3), 5–14.
- Cayan, D. R., 1992: Latent and sensible surface flux anomalies over the northern oceans: Driving the sea surface temperature. *J. Phys. Oceanogr.*, **22**, 859–881.
- Davis, R. E., 1976: Predictability of sea surface temperature and sea level pressure anomalies over the North Pacific Ocean. *J. Phys. Oceanogr.*, **6**, 249–266.
- Deser, C., and M. L. Blackmon, 1993: Surface climate variations over the North Atlantic Ocean during winter: 1900–1989. *J. Climate*, **6**, 1743–1753.
- Frankignoul, C., 1985: Sea surface temperature anomalies, planetary waves, and air-sea feedback in the middle latitudes. *Rev. Geophys.*, **23**, 357–390.
- Greatbatch, R. J., A. F. Fanning, A. D. Goulding, and S. Levitus, 1991: A diagnosis of interpentadal circulation changes in the North Atlantic. *J. Geophys. Res.*, **96**, 22 009–22 023.
- Huang, R. X., 1990: Does atmospheric cooling drive the Gulf Stream recirculation? *J. Phys. Oceanogr.*, **20**, 751–757.
- Isemer, H.-J., and L. Hasse, 1987: *The Bunker Climate Atlas of the North Atlantic Ocean*. Vol. 2: *Air-Sea Interactions*. Springer-Verlag, 252 pp.
- Kelly, K. A., 1991: The meandering Gulf Stream as seen by the Geosat altimeter: Surface transport, position and velocity variance from  $73^\circ$  to  $46^\circ\text{W}$ . *J. Geophys. Res.*, **96**, 16 721–16 738.
- , and D. R. Watts, 1994: Monitoring Gulf Stream transport by radar altimeter and inverted echo sounders. *J. Phys. Oceanogr.*, **24**, 1080–1084.
- Kushnir, Y., 1994: Interdecadal variations in North Atlantic sea surface temperature and associated atmospheric conditions. *J. Climate*, **7**, 142–157.
- , and N.-C. Lau, 1992: The general circulation model response to a North Pacific SST anomaly: Dependence on time scale and pattern polarity. *J. Climate*, **5**, 217–283.
- Lentz, S. J., 1987: A heat budget for the northern California shelf during CODE-2. *J. Geophys. Res.*, **92**, 14 491–14 509.
- Levitus, S., 1982: *Climatological Atlas of the World Ocean*. NOAA Prof. Paper No. 13, U.S. Govt. Printing Office, 173 pp.
- Lillibridge, J. L., and R. E. Cheney, 1990: Annual/interannual changes in Gulf Stream surface transport observed from Geosat. *Eos, Trans. Amer. Geophys. Union*, **71**(43), p. 1266.
- Liu, W. T., and C. Gautier, 1990: Thermal forcing on the tropical Pacific from satellite data. *J. Geophys. Res.*, **95**, 13 209–13 217.
- McCartney, M. S., and L. D. Talley, 1984: Warm to cold water conversion in the northern North Atlantic Ocean. *J. Phys. Oceanogr.*, **14**, 922–935.

- Mestas-Nuñez, A., D. B. Chelton, and M. H. Freilich, 1994: An evaluation of ECMWF-based climatological wind stress fields. *J. Phys. Oceanogr.*, **24**, 1532–1549.
- Namias, J., 1959: Recent seasonal interactions between North Pacific waters and the overlying atmospheric circulation. *J. Geophys. Res.*, **64**, 631–646.
- , 1963: Large-scale air–sea interactions over the North Pacific from summer 1962 through the subsequent winter. *J. Geophys. Res.*, **68**, 6171–6186.
- Qiu, B., 1994: Determining the mean Gulf Stream and its recirculations through combining hydrographic and altimetric data. *J. Geophys. Res.*, **99**, 951–962.
- , and K. A. Kelly, 1993: Upper-ocean heat balance in the Kuroshio Extension region. *J. Phys. Oceanogr.*, **23**, 2027–2041.
- , ———, and T. M. Joyce, 1991: Mean circulation and variability of the Kuroshio Extension from geosat altimetry data. *J. Geophys. Res.*, **96**, 18 491–18 507.
- Talley, L. D., and M. S. McCartney, 1982: Distribution and circulation of Labrador Sea Water. *J. Phys. Oceanogr.*, **12**, 1189–1205.
- Taylor, A. H., J. M. Colebrook, J. A. Stephens, and N. G. Baker, 1992: Latitudinal displacements of the Gulf Stream and the abundance of plankton in the North-East Atlantic. *J. Mar. Biol.*, **72**, 919–921.
- Worthington, L. V., 1976: On the North Atlantic circulation. *The Johns Hopkins Oceanographic Studies*, No. 6, 110 pp.
- Xue, H., J. M. Bane Jr., and L. M. Goodman, 1995: Modification of the Gulf Stream through strong air–sea interactions in winter: Observations and numerical simulations, *J. Phys. Oceanogr.*, **25**, 533–557.
- Zlotnicki, V., 1990: Sea level differences across the Gulf Stream and the Kuroshio Extension. *J. Phys. Oceanogr.*, **21**, 599–609.